Application of homomorphic theory in nonstationary deconvolution

Yanpeng Mi and Gary Margrave

ABSTRACT

Nonstationary filter theory and its application in single-trace deconvolution are reviewed. The wavelet estimation methods used in nonstationary deconvolution (NSD) are examined. As an alternative, the homomorphic method gives a good estimation of the propagating wavelet when the noise level is low and a proper low pass filter in the quefrency domain is applied. A reformulation of nonstationary deconvolution using homomorphic wavelet estimation gives promising results.

INTRODUCTION

Most conventional single-trace deconvolution techniques are based on the assumption of a stationary wavelet. The wavelet is assumed stationary so that it can be removed by from the seismic trace by applying a single stationary inverse filter. Such an assumption leads to unacceptable errors when serious wavelet distortion occurs due to anelastic attenuation or nonstationary effects. We use 'propagating wavelet' to describe a model of nonstationary seismic wavelet. Low seismic quality factor (Q) and strong stratigraphic filtering effects cause serious nonstationary wavelet distortion. This can only be handled well by a proper nonstationary inverse filter. With the assumption of local minimum phase, nonstationary deconvolution (NSD) (Schoepp, 1998) handled this problem well. The propagating wavelet is estimated from the time-variant-spectrum (TVS) of a seismic trace. The inverse filter is applied in the frequency domain in the manner of nonstationary convolution.

The success of nonstationary deconvolution is dependent on how well the propagating wavelet is estimated. Following the traditional way of estimating a minimum-phase wavelet from a smoothed version of seismic trace amplitude spectrum, NSD smoothes the TVS by convolving the amplitude spectra with a 2-D boxcar smoother and then calculates the corresponding minimum-phase spectrum. The inverse filter is then calculated and applied through nonstationary filtering. As in traditional techniques, the idea behind the smoothing is to remove both the primary and multiple reflections from the amplitude spectrum, leaving only the wavelet signature. A closer examination of NSD shows that simple spectrum smoothing may not be the best method. Another approach, homomorphic method, which is capable of separating a rapidly varying component (reflectivity) from a slowly varying component (wavelet), can be a good option for wavelet estimation.

NONSTATIONARY THEORY AND NSD

The concept of nonstationary convolution and time-variant filtering were first formulated by Pan and Shin (1976) and Sheuer and Oldenburg (1988). Margrave (1998) used a more complete formulation and showed that there are two fundamental types of nonstationary filters, called nonstationary convolution and nonstationary combination. The nonstationary convolution and its Fourier counterpart can be written as:

$$g(t) = \int_{-\infty}^{+\infty} a(t-\tau,\tau)h(\tau)d\tau \quad , \tag{1}$$

and

$$G(f) = \int_{-\infty}^{+\infty} H(F)A(f, f-F)dF \quad . \tag{2}$$

The nonstationary combination in time domain and its Fourier counterpart can be written as:

$$\bar{g}(t) = \int_{-\infty}^{+\infty} a(t-\tau, t)h(\tau)d\tau \quad , \tag{3}$$

and

$$\bar{G}(f) = \int_{-\infty}^{+\infty} H(F)A(F, f-F)dF \quad , \tag{4}$$

where $h(t)$, $G(f)$ are the input signal and its Fourier transform. $a(t)$ and $A(f)$ are an arbitrary linear filter and its Fourier transform, $g(t)$ and $G(f)$ are the nonstationary convolution and its Fourier transform, while $\bar{g}(t)$ and $\bar{G}(f)$ are the nonstationary combination and its Fourier counterpart. t is the time tracking $g(t)$ or $\bar{g}(t)$, while τ is the vector tracking the running time of nonstationary filter at time t, f and F are their counterparts in Fourier domain.

Comparing the forms of nonstationary convolution and combination, it is interesting to see that equation (2) and (4) are frequency domain combination and convolution, respectively. The derivation of the above equations can be found in Margrave, 1996.

Nonstationary deconvolution (Schoepp, 1998) was developed after this theory. A seismic trace with anelastic attenuation can be modeled by the convolution of time-varying (or propagating) wavelets with a stationary reflectivity and multiple impulse responses. The concept of superposition remains valid. A simple physical model describing the noise free procedure can be written in the mixed time-frequency domain as:

$$S(t,f) = R(t,f)M(t,f)W(t,f) \quad , \tag{5}$$

where *S(t,f)* is the time-variant spectrum of output seismic trace, *R(t,f)* and *M(t,f)* delineate primary and multiple impulse responses as varying with time *t*, *W(t, f)* stands for the propagating wavelet whose absolute amplitude and frequency content y attenuate with time due to anelastic attenuation. With the assumption of minimum phase, Q attenuation (Futterman, 1962), the amplitude spectrum variation with time of the seismic trace can be written as:

$$|S(t,f)| = |R(t,f)| \, |M(t,f)| \, |W(f)| \, e^{-\pi\alpha(t,f)ft}, \tag{6}$$

where α *(t,f)* is a generalized attenuation coefficient, *W(f)* is now the original seismic source spectrum at time *t*=0. The idea behind the NSD is to design a time-variant filter which inverse w(f) and the Q effect and then apply it to the seismic data. Figure 1 illustrates how NSD recovers band-limited reflectivity. The forward nonstationary convolution is shown in figure 1 (a). The seismic trace is created by applying a forward constant Q filter (Q=40) to a minimum phase wavelet with dominant frequency of 50 Hz and then convolved with a pseudo-random reflectivity. The TVS of the synthetic seismic trace shows the attenuation of high frequency at larger travel time (figure 1 .b). The inverse filter is calculated using a 10 Hz by 1.0 s boxcar smoother on residual TVS (figure 1.c) of the seismic trace. The residual TVS is created by removing a Q=50 attenuation surface from the TVS of the seismic trace. The Q=50 attenuation surface is restored after smoothing, for the purpose of preserving the physical attenuation trend. The inverse filter and the TVS of filtered trace is shown in figure 1.d and figure 1.e. NSD is able to recover the band-limited reflectivity from the synthetic trace (figure 2)

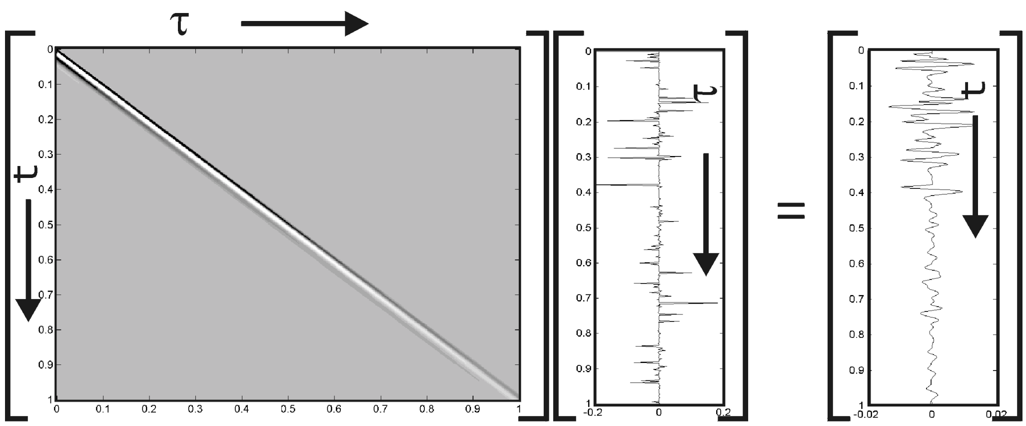

(a) Synthetic seismic trace is created by multiplication of a time-variant wavelet matrix with stationary reflectivity.

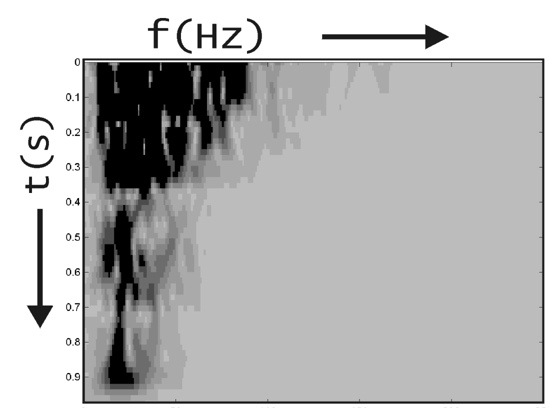

(b)TVS of the synthetic trace.

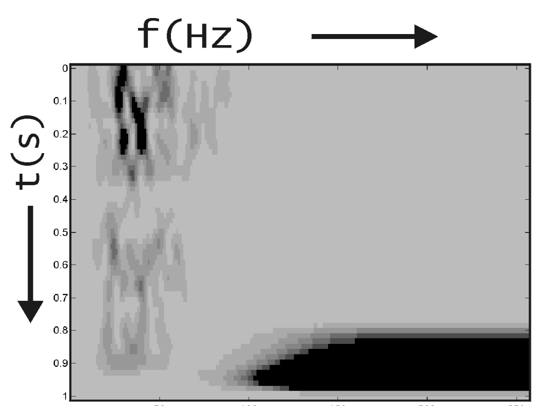

(c) Smoothed residual TVS. A constant Q=50 decay surface is removed.

Figure 1

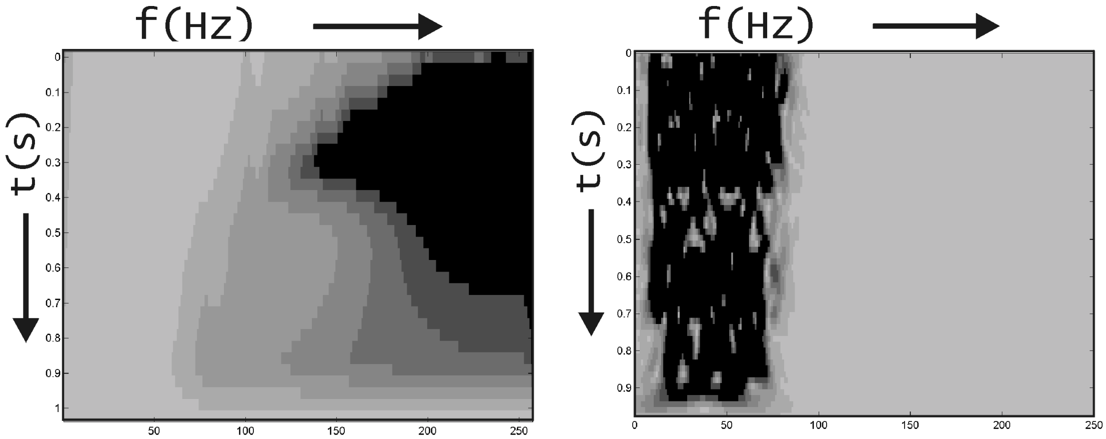

(d) Inverse of smoothed TVS. (e) TVS of deconvolved seismic trace.

Figure 1. Frequency domain operator of NSD on a synthetic seismic trace.

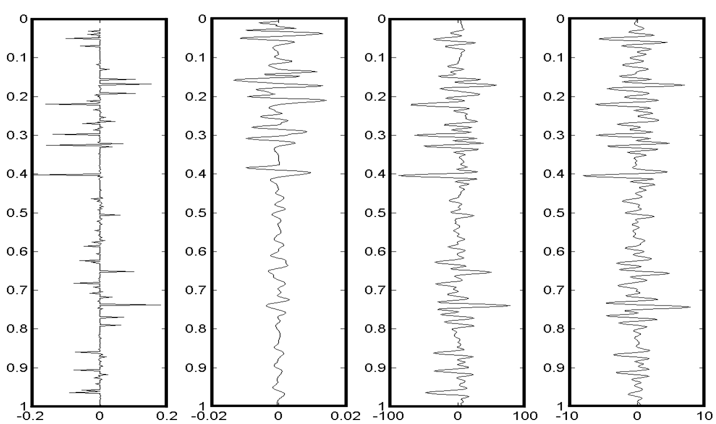

(a) (b) (c) (d)

Figure 2. NSD with 10Hz by 1.0 s boxcar smoother is able to recover the reflectivity fairly well. (a) Reflectivity, (b) synthetic trace with Q=40 attenuation, (c) band-limited reflectivity by convolving a 5-10-70-85 (same bandwidth as the deconvolved trace) ormsby wavelet with the reflectivity, (d) deconvolved trace.

HOMOMORPHIC SYSTEM AND WAVELET ESTIMATION

The essential step in NSD is the estimation of the amplitude spectrum of the propagating wavelet from the TVS. Any wavelet estimation or reflectivity removal method can be used in this process. Homomorphic method can separate a slowly varying component from a rapidly varying component in a convolution model. A nonstationary seismic trace satisfies a nonstationary convolution model and homomorphic theory can be applied locally to each time of the TVS.

The application of homomorphic theory on seismic deconvolution has been examined by several authors in 70's and 80's. fundamental papers include Ulrych, (1971); Stoffa et al., (1974); Buhl et al, (1974). However, the original idea of converting filtering in the time domain to simpler windowing in the quefrency domain, is given by Oppenheim (1965a, 1965b). Oppenheim et al. (1968) and Schafer (1969) applied homomorphic deconvolution in echo removal and found this method offered a considerable advantage that less assumption about the nature of seismic wavelet or the reflectivity is necessary. This method as applied in the estimation of propagating seismic wavelet was further addressed by Ulrych, (1971). Stoffa et al. (1974) and Buhl et al. (1974) developed the theory for water-bottom multiple attenuation using homomorphic deconvolution. However, it is a common conclusion that the deconvolved result is severely degraded when the signal-to-noise ratio is not high enough and the reflectivity sequence is not minimum phase.

I Homomorphic characterization system

Using the Z-transform, Schafer (1969) gave the following three steps to define the complex cepstrum for discrete functions of unit sample interval,

$$X(z) = \sum_{t=-\infty}^{+\infty} x(t) z^{-t}, z = e^{\sigma + i\omega}, \tag{7.a}$$

$$\hat{X}(z) = \log X(z) = \log|X(z)| + i \arg[X(z)], \tag{7.b}$$

$$x(T) = \frac{1}{2\pi i}\oint_c \hat{X}(z) z^{T-1} dz, T = 0, \pm 1, \pm 2, ..., \tag{7.c}$$

where x(t) is the original data, X(z) is its Z-transform and T is the pseudo time in the quefrency domain.

The three-step inverse definition to return to the time domain is:

$$\hat{X}(z) = \sum_{T=-\infty}^{+\infty} \hat{x}(t) z^{-T}, \tag{8.a}$$

$$X(z) = \exp[\hat{X}(z)], \tag{8.b}$$

$$x(t) = \frac{1}{2\pi i}\oint_{c'} X(z) z^{T-1} dz. \tag{8.c}$$

In practice, we use Fourier transform instead of Z-transform. There are several computational considerations when the input seismic trace passes through the homomorphic system,

I. The complex natural logarithm defined in equation 7.b is a multivalued function since $\arg[X(z)]$ has multiplicity of 2nπ where n=0,1,2…. Since $\hat{X}(z)$ must be continuous, $\arg[X(z)]$ can not be restricted to its principle values. Phase unwrapping should be done to convert $\arg[X(z)]$ to a continuous function so that $\hat{X}(z)$ is continuous. It is important to remove the linear phase component from the unwrapped phase prior to the computation of the complex cepstrum (Ulrych, 1971).

II. Aliasing is introduced into the complex cepstrum when the nonlinear logarithm operation of equation 7.b is followed by discrete Fourier transform (DFT). Although X(z) may be adequately sampled, the nonlinear operations, including logarithm, absolute value and arctangent introduce harmonics into $\hat{X}(z)$. Thus $\hat{X}(z)$ is under sampled when $z = e^{in2\pi/N}, n = 0, \pm1, \pm2 \ldots, \pm N/2$, as in the DFT. Since all harmonics out to infinite quefrencies or periods are present, the complex cepstrum will be nonzero out to infinity. DFT aliases the periods outside of the principal period range, $-1/2\Delta f < T \le 1/2\Delta f$, into this range. Schafer (1969) showed that weighting the input trace by a $a^{t/\Delta t}$ factor, helps to suppress the aliasing, where a is a positive number close to 1, t is the travel time and Δt is the sample rate. This reduces the high frequency fluctuation in $\hat{X}(z)$, thus the high frequency harmonic noise generated from the nonlinear operations are reduced. In practice, we use the Fourier transform instead of the Z-transform.

II Homomorphic deconvolution and wavelet estimation

After transforming the input seismic trace into complex cepstrum, the deconvolution in the time domain becomes the removal of the low quefrency part. This is because the slowly varying wavelet spectrum has low quefrency values. Ulrych (1971) gave some fundamental examples on the separation of wavelet and reflectivity in the quefrency domain using simple windowing. Figure 3 shows the recovery of a simple four-point minimum-phase reflectivity series and a wavelet from their convolutions. The cases of zero-phase wavelet (figure 3.a), minimum-phase wavelet (figure 3.b) and mixed phase wavelet (figure 3.c) are also shown. The zero phase wavelet is the best recovered, since the wavelet and reflectivity component are well separated in the complex cepstrum. In the case of minimum-phase wavelet, the quality is good, but slightly inferior to that of the zero-phase case. The major part of the wavelet energy is still confined near the origin but a small amount of energy is spreaded throughout the complex cepstrum. This leads to inaccuracy in wavelet estimation. Obviously, the mixed-phase case is the worst. The cepstrum near the origin now has combined contribution from the wavelet and reflectivity. The estimated wavelet does not resemble the original wavelet very well, neither does the estimated reflectivity resemble the real reflectivity. Note that the wavelet used in this case is close to maximum-phase. It is generally true that with minimum-phase reflectivity, the closer the wavelet resembles a zero-phase wavelet, the better the result that can be obtained from homomorphic deconvolution.

The reason of focusing on the minimum-phase case is that minimum-phase deconvolution or wavelet estimation is perhaps still the most important among the deconvolution methods. To get fair result as shown in figure 3.a or 3.b, the requirement of a minimum-phase reflectivity must be satisfied. Weighting the trace with a factor of a^n can convert the reflectivity sequence into minimum-phase, where a is slightly less than 1, n=t/Δt, Δt is the trace sample rate. Figure 4 and figure 5 show the effect of exponential weighting in the zero-phase and minimum-phase case. Homomorphic deconvolution can not recover either the wavelet or the reflectivity without the weighting. It is generally true that for the same nonminimum-phase reflection sequence, the a for minimum-phase wavelet should be slightly smaller than that for the case of zero-phase wavelet. The weighting factor used in figure 4 and 5 are 0.992 and 0.97, respectively.

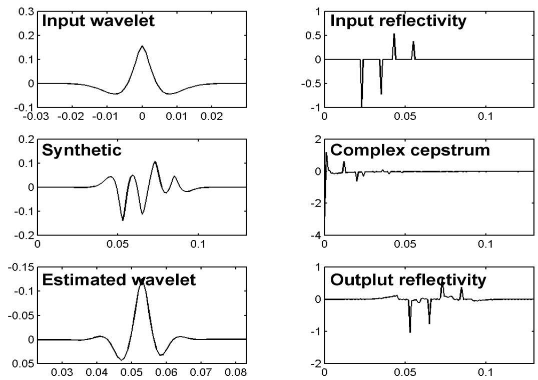

(a)Homomorphic deconvolution recovers both the reflectivity and the input zero-phase wavelet very well.

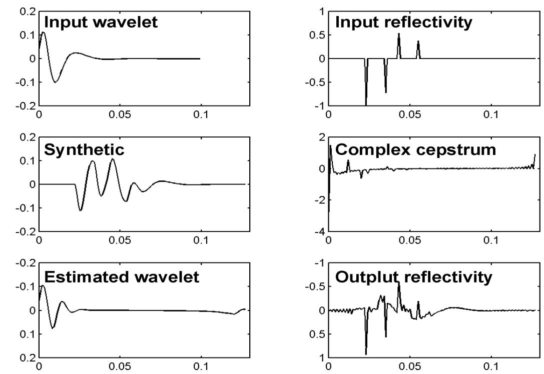

(b)Homomorphic deconvolution generates fair results in the case of a minimum-phase wavelet.

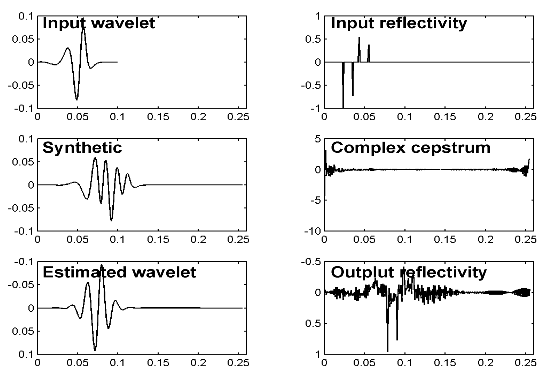

(c)Homomorphic deconvolution does not perform well for a mixed phase wavelet. Neither the estimated wavelet nor the reflectivity resembles the input.

Figure 3. Homomorphic deconvolution performance in the case of zero-phase wavelet, minimum-phase wavelet and mixed-phase wavelet.

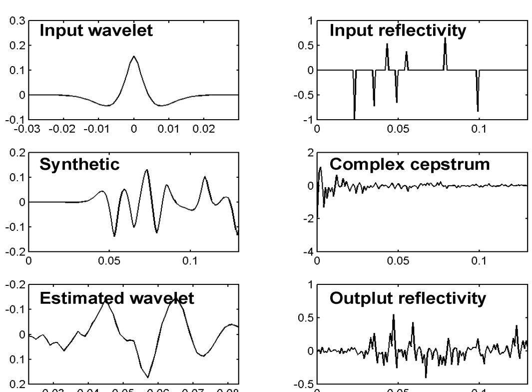

(a) Without weighting

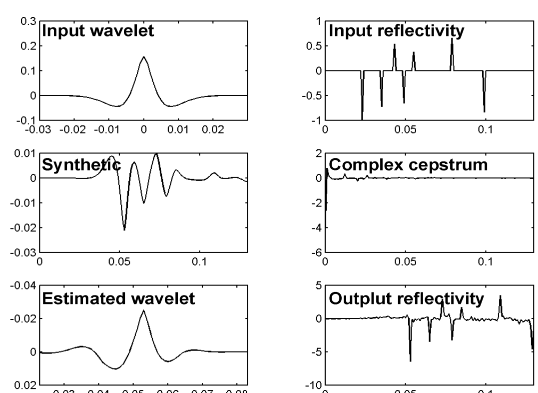

(b) Weighted by $0.992^{t/dt}$

Figure 4. Homomorphic deconvolution works well when the trace is scaled by a factor of $0.992^{t/dt}$. There is a delay of half wavelength between the original and the result.

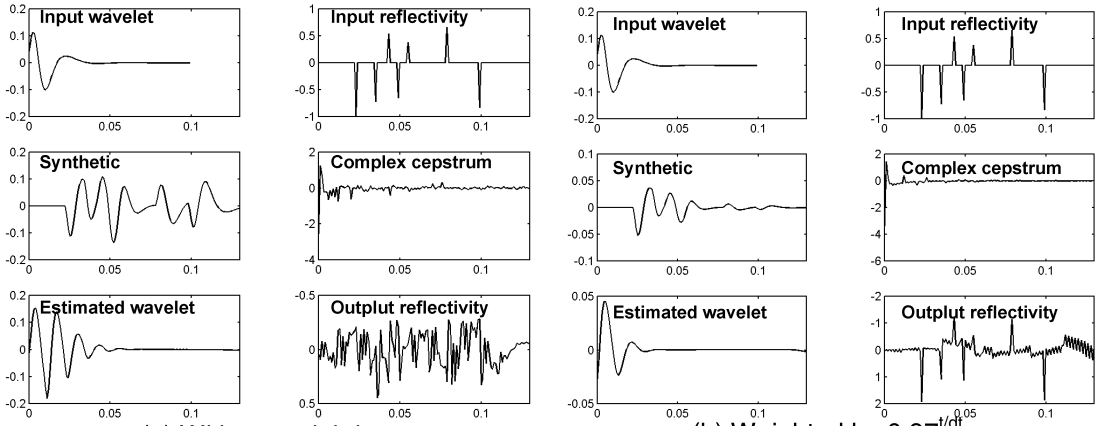

(a) Without weighting. (b) Weighted by $0.97^{t/dt}$.

Figure 5. Homomorphic deconvolution works well when the trace is scaled by a factor of $0.97^{t/dt}$ in the case of minimum-phase wavelet. No time delay between the original and the result.

HOMOMORPHIC WAVELET ESTIMATION IN NONSTATIONARY DECONVOLUTION

I. Propagating wavelet estimation

The idea of applying homomorphic method in nonstationary deconvolution is a rather direct extension of the methodology of eliminating the reflectivity from the TVS so that the propagating wavelet is recovered and the its inverse can be calculated. In the following sections we will use homomorphic nonstationary deconvolution (HNSD) for this new method.

HNSD used the same windowing methods as NSD to calculate the TVS. However, the data within each sliding time windows are scaled by an exponential decaying function (as described in the above section), starting from the beginning of the time windows. Instead of computing the TVS and then removing the reflectivity by 2-D smoothing, HNSD uses both the amplitude and phase to calculate the cepstrum of the sliding time window. A simple windowing in quefrency domain is performed to retrieve those samples belonging to the wavelet, or, in the other words, remove those samples belonging to the reflectivity. The wavelet samples are then Fourier transformed and the logarithm operation is compensated by exponential operation. We found that at this stage we have to again utilize the local minimum-phase wavelet assumption since the returned phase of the wavelet is highly unstable. This is due partly to the white noise added into the power spectrum when the logarithm operation was performed, and partly to inaccurate windowing in the quefrency domain. Although the wavelet component is close to the origin of the cepstrum, it still has some overlap with the reflectivity. An error of one or two samples of the filter length can lead to rather large phase contamination in the Fourier domain. However, the filtering error has less impact on the wavelet amplitude spectrum. A minimum-phase assumption is probably still the best in estimation for wavelet phase estimation. After extracting the propagating wavelet from the sliding time windows, a small 2-D smoother was still required to remove the residual reflectivity. The inverse is computed and applied in the same fashion as that of NSD.

II Comparison of the results from HNSD and NSD

Figure 6 shows the TVS of the propagating wavelets, estimated from homomorphic method, its inverse and the TVS of the deconvolved seismic trace.

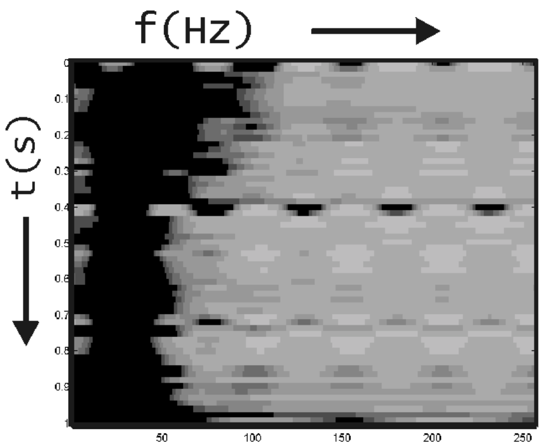

(a)TVS of propagating wavelet estimated from homomorphic method.

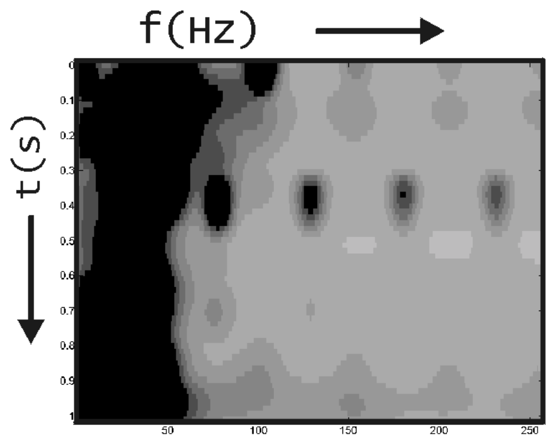

(b) Smoothed version of (a). Box car smoother: 5Hz by 0.3 s.

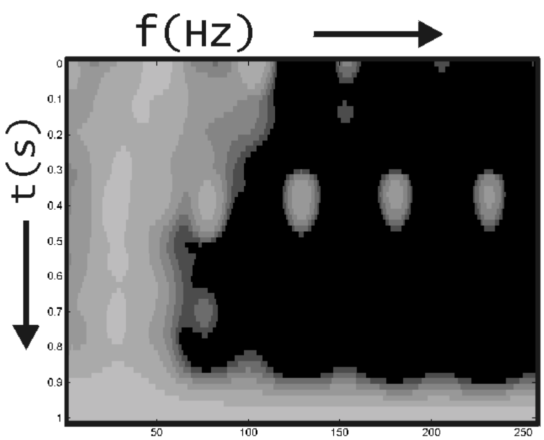

(c) Inverse of (b).

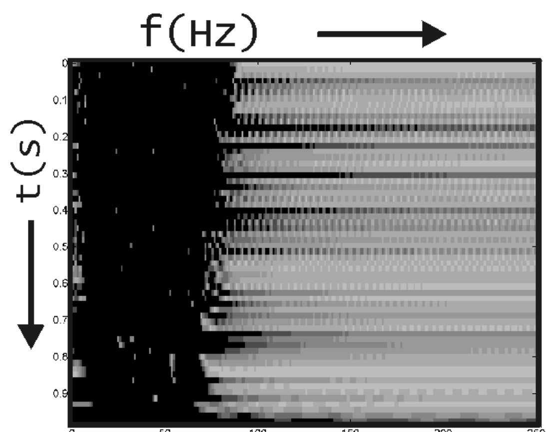

(d) TVS of deconvolved trace.

Figure 6. TVS of the propagating wavelets, estimated from homomorphic method, its inverse and the TVS of the deconvolved seismic trace.

Wavelet estimation is strongly degraded at 0.4 s and 0.7 s. Strong spikes distribute regularly in the high frequency band, roughly at 75 Hz, 125 Hz, 175 Hz and 225 Hz at 0.4 s. The same effect appears in the second time window, however, much weaker. This is due to the exponential decay scaling failing to convert the reflectivity within the time windows to minimum-phase, because large reflection coefficients exist at the end of the time windows. A 2D boxcar smoother is used to reduce this local effect. The small troughs in the TVS of the inverse filter is an immediate consequence of this effect. The TVS of HNSD processed trace is also shown in figure 6. It has the same band width as that of the NSD processed trace, while it is 'whiter' than that of NSD. The roughness of TVS outside the valid band width is because that each sliding time window has different noise level.

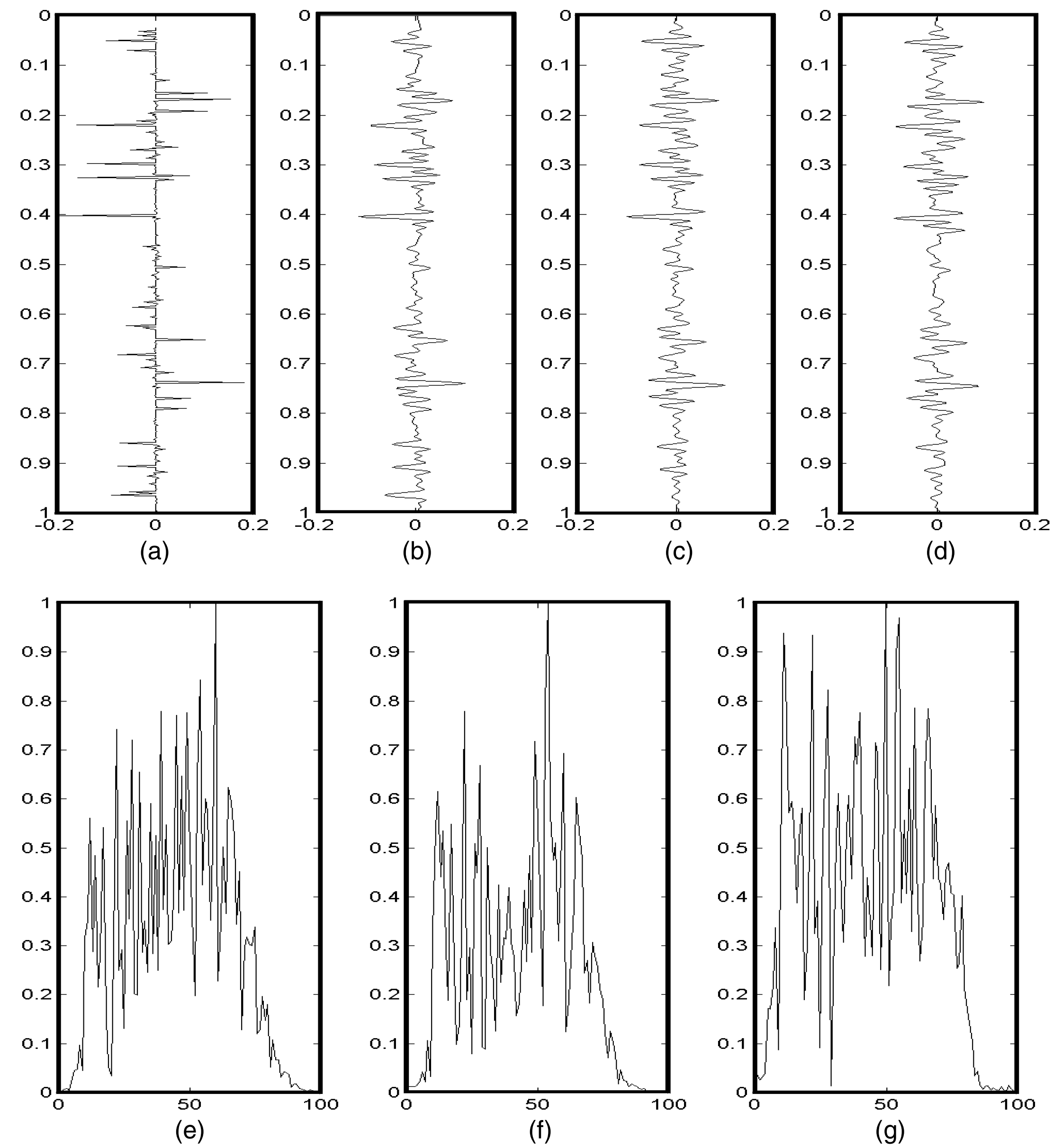

Figure 7. Comparison between the band-limited reflectivity, NSD and HNSD processed results. (a) Original reflectivity, (b) Band-limited reflectivity, (c) NSD processed trace, (d) HNSD processed trace, (e) amplitude spectrum of band limited reflectivity, (f) amplitude spectrum of NSD processed trace, (g) amplitude spectrum of HNSD processed trace.

Figure 7 shows the comparison between the band-limited reflectivity, NSD processed and HNSD processed seismic trace. The band-limited reflectivity is created by convolving the reflectivity with an ormsby filter, which has the same bandwidth as the deconvolved seismic trace. Both the NSD and HNSD processed trace are quite good. However, the amplitude spectrum of the HNSD processed traces is better whitened than that of the NSD processed trace. The notch at 45 Hz for the NSD case is not found in the HNSD result.

DISCUSSIONS AND CONCLUSIONS

The quality of HNSD process is comparable to NSD. This can be easily seen in both the time domain and the frequency domain. However, testing suggests that HNSD may give a better amplitude spectrum than NSD. However, HNSD is more sensitive to the parameters related to the homomorphic system. The nature of reflectivity is also an important issue in homomorphic wavelet estimation. Before HNSD is applied, the following issues should be considered,

1) Exponential decay scaling. For random reflectivity without strong reflection coefficient, an exponential decay parameter slightly less than 1 should be enough to generate a minimum phase reflectivity sequence. However, this exponential gain fails when a large reflection coefficient exists at the end of a sliding time window, which makes it difficult to estimate a wavelet by a simple quefrency domain windowing.

2) The design of the windowing filter in the quefrency domain is the most crucial step, and the deconvolution result is highly sensitive to this filter since a small error can be exponentially magnified in the frequency domain. Figure 8 shows how the results can vary when the filter varies from 11 to 13 with other parameters kept all the same. As we can see that 12 is the optimum filter. Both 11 and 13 gave less satisfactory results.

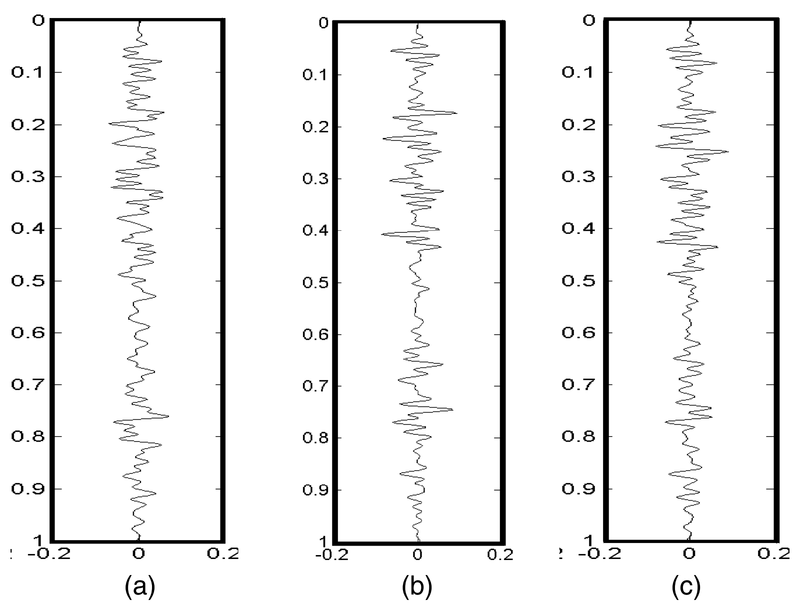

Figure 8. HNSD is sensitive to windowing in the quefrency domain. One sample away from the optimum value (12) gives degraded results. (a) 11 sample window filter, (b) 12 sample window filter, (c) 13 sample window filter.

3) Since additive noise in the time domain has tremendous negative impact on traditional homomorphic deconvolution, it is important to examine how robust HNSD when additive noise is present. Figure 9 shows the comparison of HNSD and NSD when 10% and 30 % additive noise is present in the synthetic seismic trace. NSD and HNSD generate similar results, which suggests that HNSD is at least as robust as NSD in dealing with additive noise.

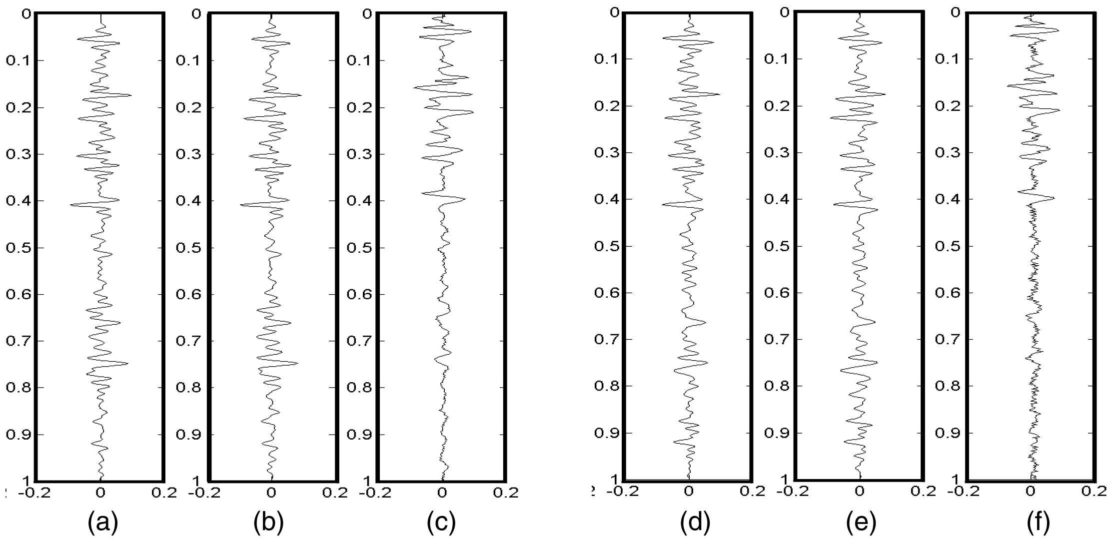

Figure 9. HNSD and NSD generate similar degraded results at the presence of 10% (a,b,c) and 30% (d,e,f) random noise. (a) NSD result, (b)HNSD result, (c) original trace plus 10% random noise, (d) NSD result, (e) HNSD result, (f) original trace plus 30% random noise.

HNSD is a simple extension of nonstationary deconvolution. Potentially all wavelet estimation methods can be incorporated with nonstationary deconvolution. There are many possibilities to improve this deconvolution method.

ACKNOWLEDGEMENT

We would like to thank the CREWES sponsors for their support.

REFERENCE

Buhl, P., Stoffa, P.L. and Bryan, G.M., 1974, The application of homomorphic deconvolution to shallow-water marine seismology-part II: real data, Geophysics, **39**, 417-426.

Futterman, W.I., 1962, Dispersive body waves, J. Geophys. Res., **73**, 3917-3935.

Margrave, G.F., 1996, Theory of nonstationary linear filtering in the Fourier domain with application to time-variant filtering, Geophysics, **63**, 244-259.

Oppenheim, A.V., 1965a, Superposition in a class of non-linear systems, Research Lab. of Electronics MIT, Tech. Rep., 432.

Oppenheim, A.V., 1965b, Optimum homomorphic filters, Research Lab. of Electronics MIT, Quart. Prog. Rep., **77**, 248-260.

Pann, K. and Shin, Y, 1976, A class of convolutional time-variiying filters, Geophysics, **41**, 28-43.

Schoepp, A.R., 1998, Nonstationary deconvolution, Master's thesis, Geology and geophysics, University of Calgary.

Sheuer, T., and Oldenburg, D.W. , 1988, Aspects of time-variant filtering, Geophysics, **53**, 1399-1409.

Schafer, R.W., 1969, Echo removal by discrete generalized linear filtering: Research Lab. of Electronics MIT, Tech. Rep. 466.

Stoffa, P.L., Buhl, P. and Bryan, G.M., 1974, The application of homomorphic deconvolution to shallow-water marine seismology-part I: models, Geophysics, **39**, 401-416.

Ulrych, T.J., 1971, Application of homomorphic deconvolution to seismology, Geophysics, **36**, 650-660.